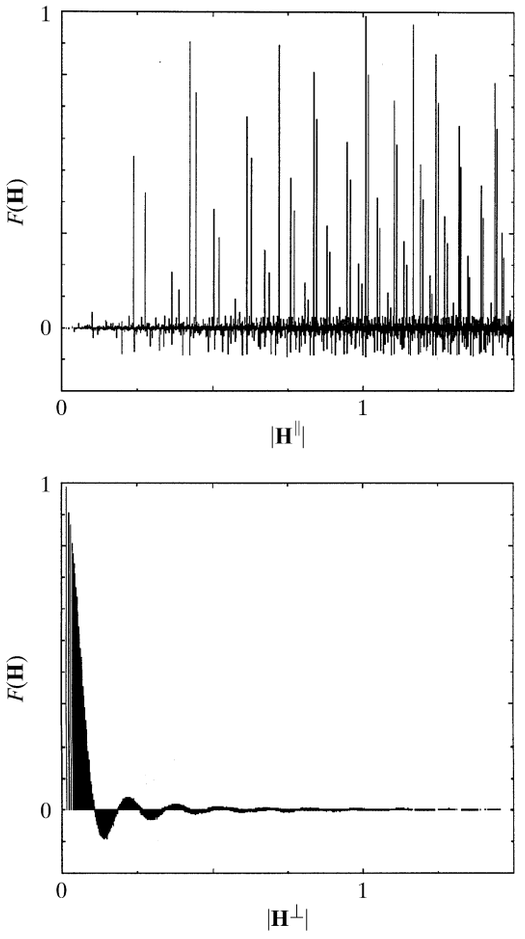

Fig. 4.6.3.35. Radial distribution function of the structure factors $F(\mathbf{H})$ of the 3D Penrose tiling (edge lengths of the Penrose unit rhombohedra $a_r = 5.0$ Å) decorated with point atoms as a function of $|\mathbf{H}^{\parallel}|$ (above) and $|\mathbf{H}^{\perp}|$ (below). All reflections are shown within $10^{-6}|F(\mathbf{0})|^2 < |F(\mathbf{H})|^2 < |F(\mathbf{0})|^2$ and $-6 \le h_i \le 6, i = 1, \ldots, 6$.

4.6.3.3.3.3. Structure factor

The structure factor of the icosahedral phase corresponds to the Fourier transform of the 6D unit cell,

$$F(\mathbf{H}) = \sum_{k=1}^{N} f_k(\mathbf{H}^{\parallel}) T_k(\mathbf{H}^{\parallel}, \mathbf{H}^{\perp}) g_k(\mathbf{H}^{\perp}) \exp(2\pi i \mathbf{H} \cdot \mathbf{r}_k),$$

with 6D diffraction vectors $\mathbf{H} = \sum_{i=1}^{6} h_i \mathbf{d}_i^*$, parallel-space atomic scattering factor $f_k(H^{\parallel})$, temperature factor $T_k(\mathbf{H}^{\parallel}, \mathbf{H}^{\perp})$ and perpendicular-space geometric form factor $g_k(\mathbf{H}^{\perp})$. $T_k(\mathbf{H}^{\parallel}, \mathbf{0})$ is equivalent to the conventional Debye–Waller factor and $T_k(\mathbf{0}, \mathbf{H}^{\perp})$ describes random fluctuations in perpendicular space. These fluctuations cause characteristic jumps of vertices (*phason flips*) in the physical space. Even random phason flips map the vertices onto positions that can still be described by physical-space vectors of the type $\mathbf{r} = \sum_{i=1}^{6} n_i \mathbf{a}_i$. Consequently, the set $M = \{\mathbf{r} = \sum_{i=1}^{6} n_i \mathbf{a}_i | n_i \in \mathbb{Z}\}$ of all possible vectors forms a $\mathbb{Z}$ module. The shape of the atomic surfaces corresponds to a selection rule for the positions actually occupied. The geometric form factor $g_k(\mathbf{H}^{\perp})$ is equivalent to the Fourier transform of the *atomic surface*, *i.e.* the 3D perpendicular-space component of the 6D *hyperatoms*.

For the example of the canonical 3D Penrose tiling, $g_k(\mathbf{H}^{\perp})$ corresponds to the Fourier transform of a triacontahedron:

$$g_k(\mathbf{H}^{\perp}) = (1/A_{\rm UC}^{\perp}) \int_{A_k} \exp(2\pi i \mathbf{H}^{\perp} \cdot \mathbf{r})\, \mathrm{d}\mathbf{r},$$

where $A_{\rm UC}^{\perp}$ is the volume of the 6D unit cell projected upon $\mathbf{V}^{\perp}$ and A_k is the volume of the triacontahedron. $A_{\rm UC}^{\perp}$ and A_k are equal in the present case and amount to the volumes of ten prolate and ten oblate rhombohedra: $A_{\rm UC}^{\perp} = 8a_r^3[\sin(2\pi/5) + \sin(\pi/5)]$. Evaluating the integral by decomposing the triacontahedron into trigonal pyramids, each one directed from the centre of the triacontahedron to three of its corners given by the vectors $\mathbf{e}_i$, $i = 1, \ldots, 3$, one obtains

$$g(\mathbf{H}^{\perp}) = (1/A_{\rm UC}^{\perp}) \sum_{R} g_k(R^T \mathbf{H}^{\perp}),$$

with $k = 1, \ldots, 60$ running over all site-symmetry operations R of the icosahedral group,

$$\begin{aligned} g_k(\mathbf{H}^{\perp}) = -iV_r[&A_2A_3A_4 \exp(iA_1) + A_1A_3A_5 \exp(iA_2) \\ &+ A_1A_2A_6 \exp(iA_3) + A_4A_5A_6] \\ &\times (A_1A_2A_3A_4A_5A_6)^{-1}, \end{aligned}$$

$A_j = 2\pi \mathbf{H}^{\perp} \cdot \mathbf{e}_j$, $j = 1, \ldots, 3$, $A_4 = A_2 - A_3$, $A_5 = A_3 - A_1$, $A_6 = A_1 - A_2$ and $V_r = \mathbf{e}_1 \cdot (\mathbf{e}_2 \times \mathbf{e}_3)$ the volume of the parallelepiped defined by the vectors $\mathbf{e}_i$, $i = 1, \ldots, 3$ (Yamamoto, 1992*b*).

4.6.3.3.3.4. Intensity statistics

The radial structure-factor distributions of the 3D Penrose tiling decorated with point scatterers are plotted in Fig. 4.6.3.35 as a function of parallel and perpendicular space. The distribution of $|F(\mathbf{H})|$ as a function of their frequencies clearly resembles a centric distribution, as can be expected from the centrosymmetric unit cell. The shape of the distribution function depends on the radius of the limiting sphere in reciprocal space. The number of weak reflections increases as the power 6, that of strong reflections only as the power 3 (strong reflections always have small $\mathbf{H}^{\perp}$ components).

The weighted reciprocal space of the 3D Penrose tiling contains an infinite number of Bragg reflections within a limited region of the physical space. Contrary to the diffraction pattern of a periodic structure consisting of point atoms on the lattice nodes, the Bragg reflections show intensities depending on the perpendicular-space components of their diffraction vectors.

4.6.3.3.3.5. Relationships between structure factors at symmetry-related points of the Fourier image

The weighted 3D reciprocal space $M^* = \{\mathbf{H}^{\parallel} = \sum_{i=1}^{6} h_i \mathbf{a}_i^* | h_i \in \mathbb{Z}\}$ exhibits the icosahedral point symmetry $K = m\bar{3}5$. It is invariant under the action of the scaling matrix S^3:

$$S = \tfrac{1}{2}\begin{pmatrix} 1 & 1 & 1 & 1 & 1 & 1 \\ 1 & 1 & 1 & -1 & -1 & 1 \\ 1 & 1 & 1 & 1 & -1 & -1 \\ 1 & -1 & 1 & 1 & 1 & -1 \\ 1 & -1 & -1 & 1 & 1 & 1 \\ 1 & 1 & -1 & -1 & 1 & 1 \end{pmatrix}_D, \quad S^3 = \begin{pmatrix} 2 & 1 & 1 & 1 & 1 & 1 \\ 1 & 2 & 1 & -1 & -1 & 1 \\ 1 & 1 & 2 & 1 & -1 & -1 \\ 1 & -1 & 1 & 2 & 1 & -1 \\ 1 & -1 & -1 & 1 & 2 & 1 \\ 1 & 1 & -1 & -1 & 1 & 2 \end{pmatrix}_D,$$

$$\begin{pmatrix} 2 & 1 & 1 & 1 & 1 & 1 \\ 1 & 2 & 1 & -1 & -1 & 1 \\ 1 & 1 & 2 & 1 & -1 & -1 \\ 1 & -1 & 1 & 2 & 1 & -1 \\ 1 & -1 & -1 & 1 & 2 & 1 \\ 1 & 1 & -1 & -1 & 1 & 2 \end{pmatrix}_D \begin{pmatrix} \mathbf{a}_1^* \\ \mathbf{a}_2^* \\ \mathbf{a}_3^* \\ \mathbf{a}_4^* \\ \mathbf{a}_5^* \\ \mathbf{a}_6^* \end{pmatrix} = \tau^3 \begin{pmatrix} \mathbf{a}_1^* \\ \mathbf{a}_2^* \\ \mathbf{a}_3^* \\ \mathbf{a}_4^* \\ \mathbf{a}_5^* \\ \mathbf{a}_6^* \end{pmatrix}.$$

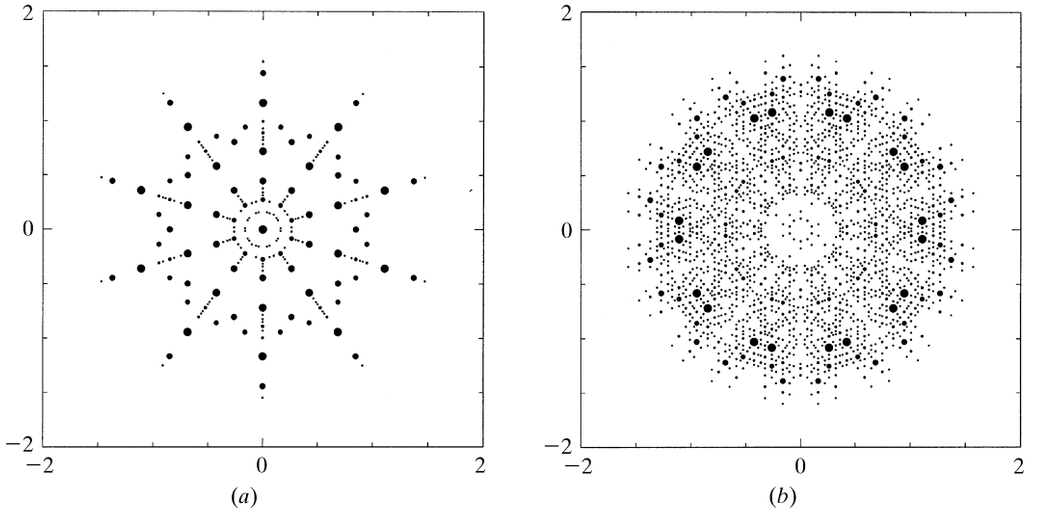

Fig. 4.6.3.36. Parallel-space distribution of (*a*) positive and (*b*) negative structure factors of the 3D Penrose tiling of the 6D *P* lattice type decorated with point atoms (edge lengths of the Penrose unit rhombohedra a_r = 5.0 Å). The magnitudes of the structure factors are indicated by the diameters of the filled circles. All reflections are shown within $10^{-4}|F(\mathbf{0})|^2 < |F(\mathbf{H})|^2 < |F(\mathbf{0})|^2$ and $-6 \le h_i \le 6, i = 1, \ldots, 6$.

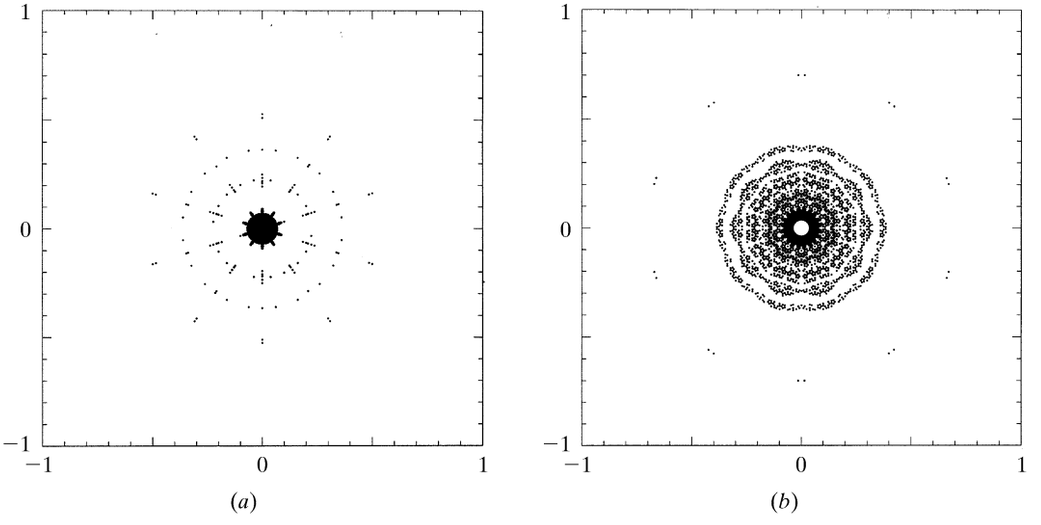

Fig. 4.6.3.37. Perpendicular-space distribution of (*a*) positive and (*b*) negative structure factors of the 3D Penrose tiling of the 6D *P* lattice type decorated with point atoms (edge lengths of the Penrose unit rhombohedra a_r = 5.0 Å). The magnitudes of the structure factors are indicated by the diameters of the filled circles. All reflections are shown within $10^{-4}|F(\mathbf{0})|^2 < |F(\mathbf{H})|^2 < |F(\mathbf{0})|^2$ and $-6 \le h_i \le 6, i = 1, \ldots, 6$.

Table 4.6.4.1. *Intensity statistics of the Fibonacci chain for a total of 161 322 reflections with* $-1000 \le h_i \le 1000$ *and* $0 \le \sin\theta/\lambda \le 2$ Å^{-1}

In the upper line, the number of reflections in the respective interval is given; in the lower line the partial sums $\sum I(\mathbf{H})$ of the intensities $I(\mathbf{H})$ are given as a percentage of the total diffracted intensity. The $F(00)$ reflection is not included in the sums.

	$F(\mathbf{H})/F(\mathbf{H})_{max} \ge 0.1$	$0.1 > F(\mathbf{H})/F(\mathbf{H})_{max} \ge 0.01$	$0.01 > F(\mathbf{H})/F(\mathbf{H})_{max} \ge 0.001$	$F(\mathbf{H})/F(\mathbf{H})_{max} < 0.001$
$0 \le \sin\theta/\lambda \le 0.2$ Å^{-1}	17	148	1505	14 511
$\sum I(\mathbf{H})$	52.53%	2.56%	0.27%	0.03%
$0.2 \le \sin\theta/\lambda \le 0.4$ Å^{-1}	11	107	1066	14 998
$\sum I(\mathbf{H})$	27.03%	2.03%	0.19%	0.02%
$0.4 \le \sin\theta/\lambda \le 0.6$ Å^{-1}	9	64	654	15 456
$\sum I(\mathbf{H})$	9.84%	0.96%	0.12%	0.01%
$0.6 \le \sin\theta/\lambda \le 0.8$ Å^{-1}	6	27	326	15 823
$\sum I(\mathbf{H})$	2.94%	0.34%	0.07%	0.01%
$0.8 \le \sin\theta/\lambda \le 2$ Å^{-1}	1	35	338	96 720
$\sum I(\mathbf{H})$	0.23%	0.79%	0.06%	0.01%
Total sum	44	381	3389	157 508
	92.57%	6.67%	0.70%	0.06%

The scaling transformation $(S^{-3})^T$ leaves a primitive 6D reciprocal lattice invariant as can easily be seen from its application on the indices:

$$\begin{pmatrix} h_1' \\ h_2' \\ h_3' \\ h_4' \\ h_5' \\ h_6' \end{pmatrix} = \begin{pmatrix} -2 & 1 & 1 & 1 & 1 & 1 \\ 1 & -2 & 1 & -1 & -1 & 1 \\ 1 & 1 & -2 & 1 & -1 & -1 \\ 1 & -1 & 1 & -2 & 1 & -1 \\ 1 & -1 & -1 & 1 & -2 & 1 \\ 1 & 1 & -1 & -1 & 1 & -2 \end{pmatrix}_D \begin{pmatrix} h_1 \\ h_2 \\ h_3 \\ h_4 \\ h_5 \\ h_6 \end{pmatrix}.$$

The matrix $(S^{-1})^T$ leaves $M^* = \{\mathbf{H}^{\parallel} = \sum_{i=1}^{6} h_i \mathbf{a}_i^* | h_i \in \mathbb{Z}\}$ invariant,

$$\begin{pmatrix} h_1' \\ h_2' \\ h_3' \\ h_4' \\ h_5' \\ h_6' \end{pmatrix} = \tfrac{1}{2}\begin{pmatrix} -1 & 1 & 1 & 1 & 1 & 1 \\ 1 & -1 & 1 & -1 & -1 & 1 \\ 1 & 1 & -1 & 1 & -1 & -1 \\ 1 & -1 & 1 & -1 & 1 & -1 \\ 1 & -1 & -1 & 1 & -1 & 1 \\ 1 & 1 & -1 & -1 & 1 & -1 \end{pmatrix}_D \begin{pmatrix} h_1 \\ h_2 \\ h_3 \\ h_4 \\ h_5 \\ h_6 \end{pmatrix},$$

for any $\mathbf{H} = \sum_{i=1}^{6} h_i \mathbf{d}_i^*$ with h_i all even or all odd, corresponding to a 6D face-centred hypercubic lattice. In a second case the sum $\sum_{i=1}^{6} h_i$ is even, corresponding to a 6D body-centred hypercubic lattice. Block-diagonalization of the matrix S decomposes it into two irreducible representations. With $WSW^{-1} = S_V = S_V^{\parallel} \oplus S_V^{\perp}$ we obtain

$$S_V = \left(\begin{array}{ccc|ccc} \tau & 0 & 0 & 0 & 0 & 0 \\ 0 & \tau & 0 & 0 & 0 & 0 \\ 0 & 0 & \tau & 0 & 0 & 0 \\ \hline 0 & 0 & 0 & -1/\tau & 0 & 0 \\ 0 & 0 & 0 & 0 & -1/\tau & 0 \\ 0 & 0 & 0 & 0 & 0 & -1/\tau \end{array}\right)_V = \left(\begin{array}{c|c} S^{\parallel} & 0 \\ \hline 0 & S^{\perp} \end{array}\right)_V,$$

the scaling properties in the two 3D subspaces: scaling by a factor τ in parallel space corresponds to a scaling by a factor $(-\tau)^{-1}$ in perpendicular space. For the intensities of the scaled reflections analogous relationships are valid, as discussed for decagonal phases (Figs. 4.6.3.36 and 4.6.3.37, Section 4.6.3.3.2.5).

4.6.4. Experimental aspects of the reciprocal-space analysis of aperiodic crystals

4.6.4.1. Data-collection strategies

Theoretically, aperiodic crystals show an infinite number of reflections within a given diffraction angle, contrary to periodic crystals. The number of reflections to be included in a structure analysis of a *periodic* crystal may be very high (one million for virus crystals, for instance) but there is no ambiguity in the selection of reflections to be collected: all Bragg reflections within a limiting sphere in reciprocal space, usually given by $0 \leq \sin\theta/\lambda \leq 0.7$ Å^{-1}, are used. All reflections, observed and unobserved, are included to fit a reliable structure model.

However, for *aperiodic* crystals it is not possible to collect the infinite number of dense Bragg reflections within $0 \leq \sin\theta/\lambda \leq 0.7$ Å^{-1}. The number of observable reflections within this limiting sphere depends only on the spatial and intensity resolution.

What happens if not all reflections are included in a structure analysis? How important is the contribution of reflections with large perpendicular-space components of the diffraction vector which are weak but densely distributed? These problems are illustrated using the example of the Fibonacci sequence. An infinite model structure consisting of Al atoms with isotropic thermal parameter $B = 1$ Å^2, and distances S = 2.5 Å and L = τS, was used for the calculations (Table 4.6.4.1).

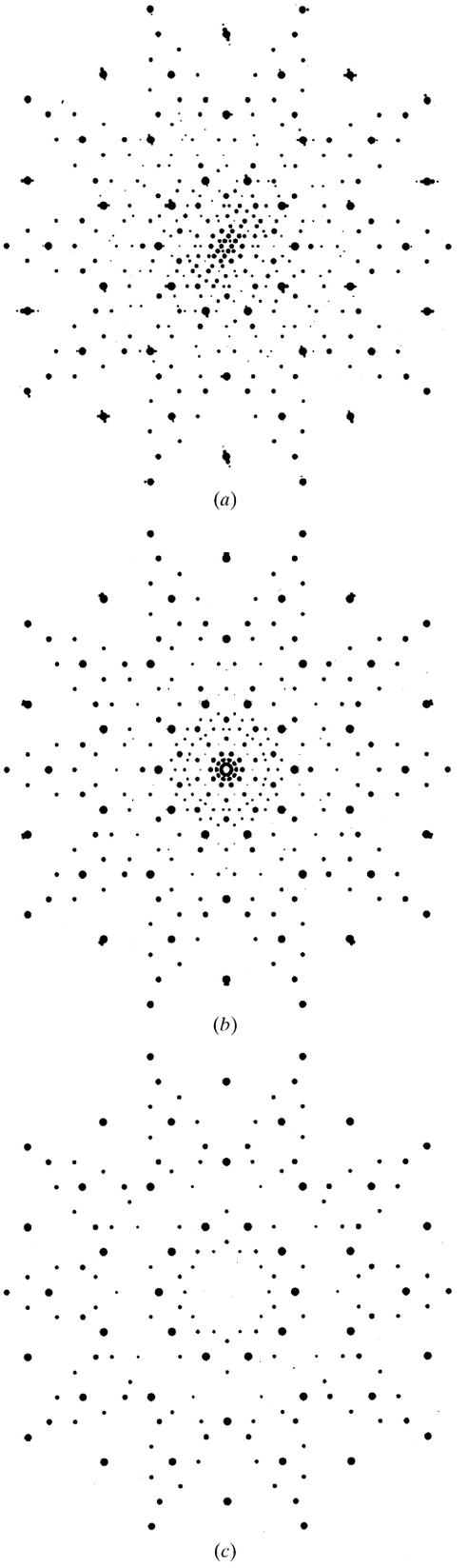

Fig. 4.6.4.1. Simulated diffraction patterns of (*a*) the $\simeq 52$ Å single-crystal approximant of decagonal Al–Co–Ni, (*b*) the fivefold twinned approximant, and (*c*) the decagonal phase itself (Estermann *et al.*, 1994).

references